

## Single-Molecule Magnets

Strong Direct Magnetic Coupling in a Dinuclear Co<sup>II</sup> Tetrazine Radical Single-Molecule MagnetToby J. Woods,<sup>[a]</sup> Maria Fernanda Ballesteros-Rivas,<sup>[a]</sup> Sergei M. Ostrovsky,<sup>[b]</sup> Andrew V. Palii,<sup>[b]</sup> Oleg S. Reu,<sup>[b]</sup> Sophia I. Klokishner,<sup>[b]</sup> and Kim R. Dunbar<sup>\*[a]</sup>

**Abstract:** The ligand-centered radical complex [(CoTPMA)<sub>2</sub>-μ-bmtz<sup>-</sup>](O<sub>3</sub>SCF<sub>3</sub>)<sub>3</sub>·CH<sub>3</sub>CN (bmtz = 3,6-bis(2'-pyrimidyl)-1,2,4,5-tetrazine, TPMA = tris-(2-pyridylmethyl)-amine) has been synthesized from the neutral bmtz precursor. Single-crystal X-ray diffraction studies have confirmed the presence of the ligand-centered radical. The Co<sup>II</sup> complex exhibits slow paramagnetic relaxation in an applied DC field with a barrier to spin reversal of 39 K. This behavior is a result of strong antiferromagnetic metal–radical coupling combined with positive axial and strong rhombic anisotropic contributions from the Co<sup>II</sup> ions.

Research on molecular magnetic materials, particularly single-molecule magnets (SMMs), is witnessing a veritable explosion of activity owing to the potential applications in high-density data storage,<sup>[1]</sup> spintronics,<sup>[2]</sup> and quantum computing.<sup>[2b,3]</sup> SMMs are well suited to these applications owing to the existence of a bistable ground state in these molecules below a certain blocking temperature ( $T_b$ ) which enables these molecules to behave as tiny bar magnets of precisely defined size and shape. One of the major challenges facing this field is the temperature required for the observation of magnetic bistability. One of the hurdles for achieving higher temperature SMM behavior in large polynuclear complexes is that controlling global anisotropy in these molecules is difficult owing to the unpredictable nature of the synthesis of these large molecules. An entirely different approach that is experiencing considerable success is the design of low nuclearity complexes in which a combination of geometry, coordination number, and a specific electronic configuration leads to strong single-ion anisotropy. A natural limitation of this strategy is that the total spin of the system, which also has some bearing on  $T_b$ , is limited for

smaller nuclearity compounds, but one can increase the total spin of the system by incorporating radical ligands into the molecule. For example, organic radicals in the nitroxide and verdazyl families have been used to synthesize SMMs.<sup>[4]</sup> In addition to increasing the total spin of the system, organic radical bridges have the added advantage of increasing the magnitude of the magnetic exchange coupling<sup>[5]</sup> which leads to higher blocking temperatures.<sup>[5a,b,6]</sup> A particularly impressive example of the use of radical bridging ligands is the work of Long and co-workers who reported that the N<sub>2</sub><sup>3-</sup> radical-bridged compound [K(18-crown-6)]{[(Me<sub>3</sub>Si)<sub>2</sub>N<sub>2</sub>](THF)Gd<sub>2</sub>(μ-η<sup>2</sup>:η<sup>2</sup>-N<sub>2</sub>)} exhibits a superexchange coupling constant of  $J = -27 \text{ cm}^{-1}$  between the Gd<sup>III</sup> ions—the strongest coupling observed to date for 4f spin centers.<sup>[5a]</sup> The Tb<sup>III</sup> analog of the same complex exhibits magnetic hysteresis up to 14 K,<sup>[5b]</sup> a temperature that has been rivaled by only one other molecule, namely [Er<sub>2</sub>(COT')<sub>3</sub>].<sup>[7]</sup>

Since the report of [Co<sub>4</sub>(hmp)<sub>4</sub>(MeOH)<sub>4</sub>Cl<sub>4</sub>], the first Co<sup>II</sup> complex to display SMM behavior,<sup>[8]</sup> only a few reports of multinuclear Co<sup>II</sup> exchange-coupled SMM systems have appeared in the literature.<sup>[9]</sup> The existence of mononuclear cobalt SMMs coupled to terminal radical ligands<sup>[10]</sup> inspired us to expand on this concept by using the tetrazine-based ligand 3,6-bis(2'-pyrimidyl)-1,2,4,5-tetrazine (bmtz), a ligand that is known to exist as a stable radical anion,<sup>[11]</sup> to prepare dinuclear Co<sup>II</sup> SMM complexes. Herein, we report the synthesis and characterization of [(CoTPMA)<sub>2</sub>-μ-bmtz<sup>-</sup>](O<sub>3</sub>SCF<sub>3</sub>)<sub>3</sub>·CH<sub>3</sub>CN (TPMA = tris-(2-pyridylmethyl)amine), (**1**; Figure 1). This complex displays very strong cobalt–radical exchange coupling and slow paramagnetic relaxation of the magnetization, indicative of an SMM.

Compound **1** was prepared by reacting a solution of in situ generated [Co(TPMA)(solv)<sub>2</sub>](O<sub>3</sub>SCF<sub>3</sub>)<sub>2</sub> with bmtz and Cp<sub>2</sub>Co (Cp = cyclopentadiene) in CH<sub>3</sub>CN. The cationic unit of **1** consists of two [Co(TPMA)]<sup>2+</sup> units bridged by a single bmtz radical ligand. The two cobalt fragments are arranged *anti* to each other across the bmtz ligand. The single Co ion in the asymmetric unit exhibits a distorted octahedral coordination geometry. The N<sub>py</sub>-Co-N<sub>amine</sub> angles in the Co(TPMA) moiety range from 76.12(12) to 79.16(12)°, much more acute than the expected 90° angles for a bona fide octahedral coordination geometry. The Co–N bond lengths also vary significantly, from 2.100(3) to 2.256(3) Å. This distortion is best described as a meridional elongation, in which the Co1–N8, Co1–N2, and Co1–N6 bonds form one meridian of the octahedron, spanning from the bmtz pyrimidine ring to the bridgehead amine N atom of TPMA, and one of the pyridine rings of TPMA with

[a] T. J. Woods, Dr. M. F. Ballesteros-Rivas, Dr. K. R. Dunbar  
Department of Chemistry  
Texas A&M University  
College Station, TX 77842 (USA)  
E-mail: dunbar@chem.tamu.edu  
Homepage: <http://www.chem.tamu.edu/rgroup/dunbar/>

[b] S. M. Ostrovsky, A. V. Palii, O. S. Reu, S. I. Klokishner  
Institute of Applied Physics  
Academy of Sciences of Moldova  
Academy str. 5, Kishinev, MD 2028 (Moldova)

Supporting information for this article is available on the WWW under <http://dx.doi.org/10.1002/chem.201501726>.

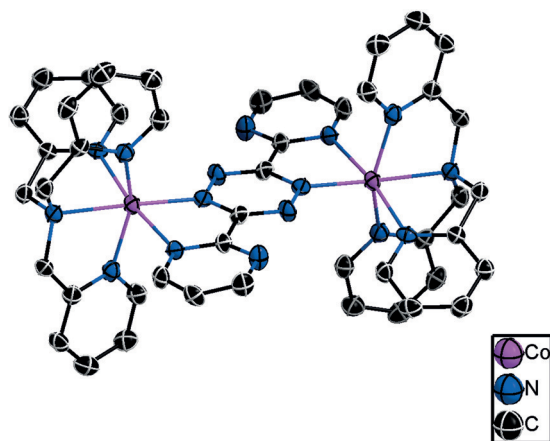


**Figure 1.** Thermal ellipsoid plot of the cationic unit of **1**. Thermal ellipsoids are drawn at the 50% probability level. H atoms were omitted for the sake of clarity.

an average bond length of 2.21 Å. The Co1–N5, Co1–N4, and Co1–N10 bonds form the other meridian of the octahedron with an average bond length of 2.08 Å. A list of selected bond lengths, angles, and an atom-numbering scheme are provided in Table S2 in the Supporting Information. Evidence for the radical anion form of the bmtz ligand is the N3–N5a distance of 1.385(4) Å in the tetrazine ring, which is significantly longer than the ~1.33 Å expected for the neutral form of the ligand and consistent with previous reports of the radical anion.<sup>[12]</sup> Moreover, charge balance requires the cationic framework to have a 3+ charge, consistent with two Co<sup>II</sup> centers and one ligand radical. The intramolecular Co–Co separation is 6.80 Å, with the closest intermolecular Co–Co contact being 8.95 Å.

The static DC magnetic properties of **1** were measured from 2–300 K in a 1000 Oe DC field (Figure 2). The  $\chi T$  value of 4.50 emu K mol<sup>-1</sup> at 300 K is slightly higher than the expected spin-only value of 4.13 emu K mol<sup>-1</sup> for an uncoupled system, suggesting that the orbital angular momentum is not fully quenched in this complex. The  $\chi T$  value exhibits a gradual increase from 300 K to ~45 K, below which temperature the

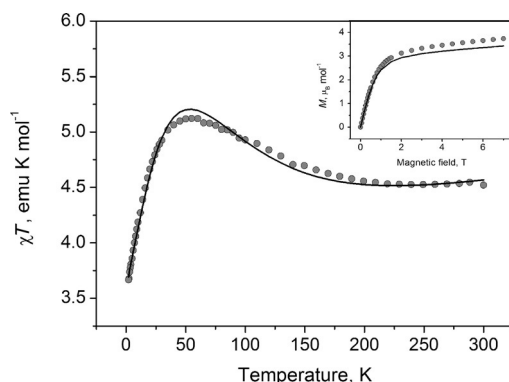


**Figure 2.** Experimental temperature dependence of  $\chi T$  for **1** measured at  $H = 1000$  Oe (circles). Inset shows the magnetization vs. field at  $T = 1.8$  K. Theoretical curves (solid lines) are calculated with  $\Delta_{ax} = 1150$  cm<sup>-1</sup>,  $\Delta_{rh} = 280$  cm<sup>-1</sup>,  $\kappa = 0.757$ , and  $J_{ex} = -62.5$  cm<sup>-1</sup>.

value decreases rapidly to a value of 3.67 emu K mol<sup>-1</sup> at 2 K. For **1** at  $T = 1.8$  K the magnetization as function of magnetic field does not saturate at 7 T and it is lower than the value of  $5 \mu_B$ , corresponding to the  $S = 5/2$  pure spin ground state that arises from antiferromagnetic coupling of the Co<sup>II</sup> ions with the bmtz radical. This indicates that the orbital magnetic moment is not fully quenched, giving rise to a significant single-ion anisotropy. Reduced magnetization data for this complex (Figure S2 in the Supporting Information) exhibit splitting of the isofield lines, consistent with an anisotropic system or low-lying excited states.

We used the following model Hamiltonian to explain the DC magnetic properties:

$$H = -\frac{3}{2} \lambda \kappa \sum_{i=1,2} I_i s_i + \Delta_{ax} \sum_{i=1,2} \left[ I_{zi}^2 - \frac{1}{3} I(i+1) \right] + \Delta_{rh} \sum_{i=1,2} (I_{xi}^2 - I_{yi}^2) - 2 J_{ex} (s_1 s_R + s_R s_2) + \mu_B \mathbf{H} \left[ \sum_{i=1,2} \left( -\frac{3}{2} \kappa I_i + g_e s_i \right) + g_e s_R \right]$$

This Hamiltonian operates within the space representing a direct product of cubic  $^4T_1$  terms (states with fictitious orbital angular momenta  $l = 1$ ) and the spin-1/2 states for the radical. The first term in  $H$  describes the spin-orbital interaction within each Co<sup>II</sup> ion; index  $i$  enumerates Co<sup>II</sup> ions,  $\lambda$  is the spin-orbit coupling parameter, and  $\kappa$  is the orbital reduction factor. The second and third terms account for the axial and rhombic components of the crystal field, where  $\Delta_{ax}$  and  $\Delta_{rh}$  are the corresponding crystal-field parameters, and  $I_{zi}$ ,  $I_{xi}$ , and  $I_{yi}$  are the components of the orbital angular momentum operator for the Co<sup>II</sup> ions. The complex is centrosymmetric and so the principal axes of the crystal-field tensors for the Co<sup>II</sup> centers are parallel and the molecular frame axes  $X$ ,  $Y$ ,  $Z$  are chosen to be parallel to these local ones. The fourth term represents the isotropic exchange interaction between the Co<sup>II</sup> ions and the radical defined in the framework of the Lines model,<sup>[13]</sup>  $J_{ex}$  is the exchange parameter. Finally, the last term represents the Zeeman interaction, including both the orbital and spin parts for the Co<sup>II</sup> ions, where  $\mu_B$  is the Bohr magneton,  $\mathbf{H}$  is the magnetic field, and  $g_e$  is the electronic Lande factor. For the spin-orbit coupling parameter we use the typical value  $\lambda = -180$  cm<sup>-1</sup>,<sup>[14]</sup> while the four parameters  $\Delta_{ax}$ ,  $\Delta_{rh}$ ,  $\kappa$ , and  $J_{ex}$  are allowed to vary during the course of the fitting procedure. The theoretical  $\chi T$  and magnetization curves obtained with the set of the best-fit parameters  $\Delta_{ax} = 1150$  cm<sup>-1</sup>,  $\Delta_{rh} = 280$  cm<sup>-1</sup>,  $\kappa = 0.757$ , and  $J_{ex} = -62.5$  cm<sup>-1</sup> are shown by solid lines in Figure 2. It is seen that this set of parameters reproduces the experimentally observed magnetic behavior of **1** quite well with the agreement criteria being equal to 0.9% and 5.8% for  $\chi T$  versus  $T$  and  $M$  versus  $H$ , respectively. The temperature dependence of the main components of the  $\chi T$  tensor calculated with the best-fit parameters (Figure 3) reveal that  $Z$  is the hard axis of magnetization. Note that this result is similar to the situation of a positive zero-field splitting parameter  $D$  in the case of pure spin systems. At the same time, the large difference between  $\chi_{xx} T$  and  $\chi_{yy} T$  components indicates the presence of strong rhombic anisotropy. At first glance, the inclusion in the

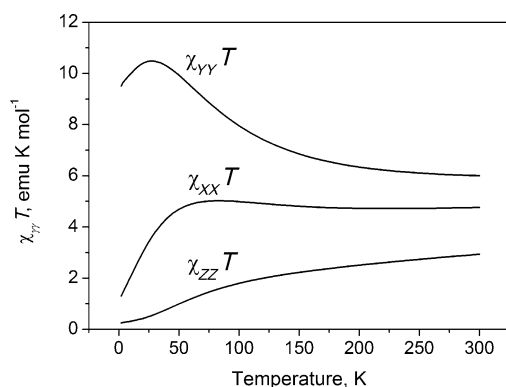


**Figure 3.** Components of the  $\chi T$  tensor calculated with  $\Delta_{ax} = 1150 \text{ cm}^{-1}$ ,  $\Delta_{rh} = 280 \text{ cm}^{-1}$ ,  $\kappa = 0.757$ , and  $J_{ex} = -62.5 \text{ cm}^{-1}$ .

fitting procedure of four adjustable parameters may lead to over-parameterization, that is, to the possibility of multiple solutions. The parameter  $J_{ex}$  is essentially uniquely determined by the position of the maximum in the  $\chi T$  versus  $T$  curve, whereas the value of the parameter  $\kappa$  was assumed to be constrained in the limits typical for the high-spin  $\text{Co}^{\text{II}}$  ion in octahedral surroundings (from 0.6 to 0.9).<sup>[13]</sup> Therefore, taking into account that we performed a simultaneous fitting of  $\chi T$  versus  $T$  and  $M$  versus  $H$  dependences, one can assert with confidence that the obtained set of the best-fit parameters is the only possible one.

At this point it is important to compare our approach with that used for the examination of the DC magnetic properties of the similar radical-bridged dinuclear  $\text{Co}^{\text{II}}$  complex  $[\text{K}(\text{DME})_4][\text{dmp}_2\text{Ni}(\text{Co}[\text{N}(\text{SiMe}_3)_2]_2)]$  ( $\text{dmp}_2\text{Ni}^{2-} = \text{bis}-(2,6\text{-dimethylphenyl})\text{-nindigo}$ ).<sup>[5d]</sup> In this work, the energy levels of single  $\text{Co}^{\text{II}}$  centers were determined from ab initio calculations of the crystal-field terms with subsequent mixing and splitting of these terms by spin-orbit coupling. In contrast, in our case, these energy patterns were modeled with the aid of the simplified single-ion Hamiltonian, which acts within the ground cubic  $^4T_1$  terms of each  $\text{Co}^{\text{II}}$  ion and contains the low-symmetry crystal field (axial and rhombic contributions) and spin-orbit coupling operators. In both of these approaches, the exchange coupling was treated in the framework of the Lines model,<sup>[13]</sup> neglecting the anisotropic orbitally dependent exchange contributions. We also neglected the rather weak Co–Co superexchange and retained only the dominant Co–radical exchange term. Therefore, in both approaches, the exchange parameters were obtained from a fitting procedure. Note that in this way the authors of ref. [5d] obtained a very strong antiferromagnetic Co–radical direct exchange of  $J = -132.74 \text{ cm}^{-1}$  (defined by the Hamiltonian  $-J \cdot s_{\text{Co}} \cdot s_{\text{R}}$ ) and a much weaker ferromagnetic Co–Co superexchange interaction.<sup>[5d]</sup> It is remarkable that this  $J$  parameter is smaller by a factor of two than that in the case of the present compound for which the Hamiltonian is defined by  $2J_{ex} = -125 \text{ cm}^{-1}$ .

Dynamic AC magnetic measurements of **1** in zero applied DC field revealed no out-of-phase signal, but in an 800 Oe DC field a prominent  $\chi''$  signal (Figure 4, top) is observed. At low temperatures, the maxima in  $\chi''$  are frequency independent

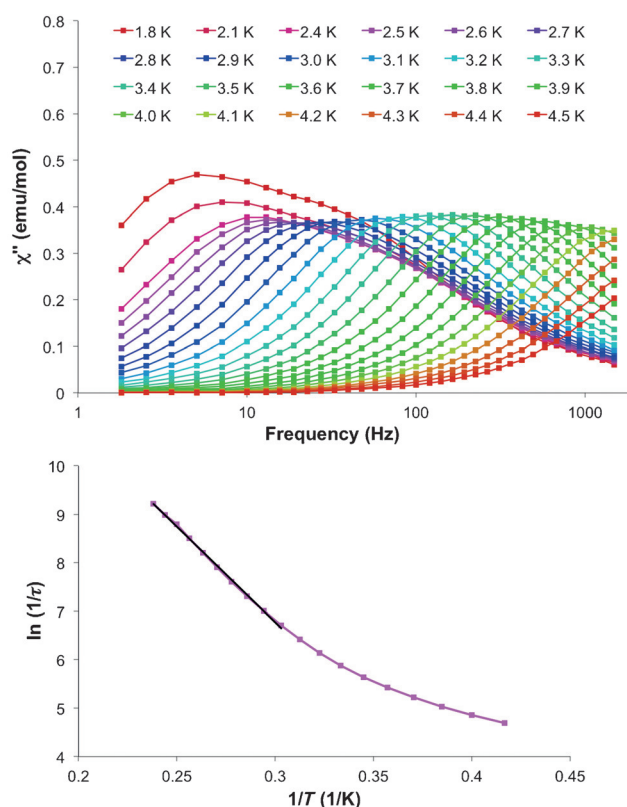


**Figure 4.** Top: Frequency dependence of **1** in an 800 Oe applied DC field. The solid lines are guides for the eye. Bottom: Arrhenius plot for **1**. The black line is a linear regression fit to the data from 3.3–4.2 K, which resulted in the barrier height and pre-exponential factor of 39 K with  $\tau_0 = 8.1 \times 10^{-9} \text{ s}$  as discussed in the text.

owing to rapid quantum tunneling, but become frequency dependent at higher temperatures, indicative of an Orbach relaxation process. We thus arrive at the conclusion that **1** belongs to a class of SMMs that display field-induced slow magnetic relaxation with axial and strong rhombic anisotropy. The Cole–Cole plot (Figure S5 in the Supporting Information) was fit with a modified Debye function<sup>[15]</sup> to extract the values of  $\tau$  and  $\alpha$ . The  $\tau$  values were used to construct an Arrhenius plot that shows two distinct regions (Figure 4, bottom). The low-temperature region exhibits non-linear behavior consistent with quantum tunneling. The linear region between 3.3 and 4.2 K, where relaxation is through an Orbach process,<sup>[16]</sup> was used to extract an energy barrier of 39 K with  $\tau_0 = 8.1 \times 10^{-9} \text{ s}$ , a slightly higher barrier than the 33 K barrier reported for  $[\text{K}(\text{DME})_4][\text{dmp}_2\text{Ni}(\text{Co}[\text{N}(\text{SiMe}_3)_2]_2)]$ .<sup>[5d]</sup> The  $\alpha$  values between 3.3 and 4.2 K are less than 0.12, indicating a narrow distribution of relaxation times.

In summary, a dinuclear radical-bridged  $\text{Co}^{\text{II}}$  compound that exhibits strong direct magnetic exchange coupling and SMM behavior has been prepared from a readily accessible ligand by self-assembly. Analogous compounds of other first-row transition metals as well as second- and third-row elements are being pursued.

## Acknowledgements

This work was supported by the National Science Foundation under Grant No. CHE-1310574. T.J.W. thanks the Department of Energy Office of Science Graduate Fellowship Program (DOE SCGF), made possible in part by the American Recovery and Reinvestment Act of 2009, administered by ORISE-ORAU under contract No. DE-AC05-06OR23100 for fellowship support. M.F.B.R. thanks the Instituto de Ciencia y Tecnología del Distrito Federal (ICyTDF) for fellowship support. S.I.K., A.V.P., S.M.O., and O.S.R. acknowledge the STCU (project N 5929) for financial support.

**Keywords:** cobalt · dinuclear single molecule magnet · magnetic exchange coupling · radicals · tetrazine

- [1] D. Gatteschi, R. Sessoli, J. Villain, *Molecular Nanomagnets*, Oxford University Press, Inc., New York, **2006**.
- [2] a) S. Sanvito, *Chem. Soc. Rev.* **2011**, *40*, 3336–3355; b) J. M. Clemente-Juan, E. Coronado, A. Gaita-Arino, *Chem. Soc. Rev.* **2012**, *41*, 7464–7478.
- [3] F. Troiani, M. Affronte, *Chem. Soc. Rev.* **2011**, *40*, 3119–3129.
- [4] I. Ratera, J. Veciana, *Chem. Soc. Rev.* **2012**, *41*, 303–349.
- [5] a) J. D. Rinehart, M. Fang, W. J. Evans, J. R. Long, *Nat. Chem.* **2011**, *3*, 538–542; b) J. D. Rinehart, M. Fang, W. J. Evans, J. R. Long, *J. Am. Chem. Soc.* **2011**, *133*, 14236–14239; c) M. Zhu, Y.-G. Li, Y. Ma, L.-C. Li, D.-Z. Liao, *Inorg. Chem.* **2013**, *52*, 12326–12328; d) S. Fortier, J. J. Le Roy, C.-H. Chen, V. Vieru, M. Murugesu, L. F. Chibotaru, D. J. Mindiola, K. G. Caulton, *J. Am. Chem. Soc.* **2013**, *135*, 14670–14678; e) J. Wu, D. J. MacDonal, R. Clérac, I.-R. Jeon, M. Jennings, A. J. Lough, J. Britten, C. Robertson, P. A. Dube, K. E. Preuss, *Inorg. Chem.* **2012**, *51*, 3827–3839; f) I.-R. Jeon, J. G. Park, D. J. Xiao, T. D. Harris, *J. Am. Chem. Soc.* **2013**, *135*, 16845–16848.
- [6] S. Demir, J. M. Zadrozny, M. Nippe, J. R. Long, *J. Am. Chem. Soc.* **2012**, *134*, 18546–18549.
- [7] J. J. Le Roy, L. Ungur, I. Korobkov, L. F. Chibotaru, M. Murugesu, *J. Am. Chem. Soc.* **2014**, *136*, 8003–8010.
- [8] E. C. Yang, D. N. Hendrickson, W. Wernsdorfer, M. Nakano, L. N. Zakharov, R. D. Sommer, A. L. Rheingold, M. Ledezma-Gairaud, G. Christou, *J. Appl. Phys.* **2002**, *91*, 7382–7384.
- [9] a) M. Murrie, S. J. Teat, H. Stoeckli-Evans, H. U. Güdel, *Angew. Chem. Int. Ed.* **2003**, *42*, 4653–4656; *Angew. Chem.* **2003**, *115*, 4801–4804; b) D. E. Freedman, M. V. Bennett, J. R. Long, *Dalton Trans.* **2006**, 2829–2834; c) Y. Song, P. Zhang, X.-M. Ren, X.-F. Shen, Y.-Z. Li, X.-Z. You, *J. Am. Chem. Soc.* **2005**, *127*, 3708–3709; d) D. Yoshihara, S. Karasawa, N. Koga, *J. Am. Chem. Soc.* **2008**, *130*, 10460–10461; e) Y. Liu, Z. Chen, J. Ren, X.-Q. Zhao, P. Cheng, B. Zhao, *Inorg. Chem.* **2012**, *51*, 7433–7435; f) K. C. Mondal, A. Sundt, Y. Lan, G. E. Kostakis, O. Waldmann, L. Ungur, L. F. Chibotaru, C. E. Anson, A. K. Powell, *Angew. Chem. Int. Ed.* **2012**, *51*, 7550–7554; *Angew. Chem.* **2012**, *124*, 7668–7672; g) G. P. Guedes, S. Soriano, L. A. Mercante, N. L. Speziali, M. A. Novak, M. Andruh, M. G. F. Vaz, *Inorg. Chem.* **2013**, *52*, 8309–8311; h) M. Towatari, K. Nishi, T. Fujinami, N. Matsumoto, Y. Sunatsuki, M. Kojima, N. Mochida, T. Ishida, N. Re, J. Mrozinski, *Inorg. Chem.* **2013**, *52*, 6160–6178; i) T. Yamaguchi, J.-P. Costes, Y. Kishima, M. Kojima, Y. Sunatsuki, N. Bréfuel, J.-P. Tuchagues, L. Vendier, W. Wernsdorfer, *Inorg. Chem.* **2010**, *49*, 9125–9135.
- [10] a) S. Kanegawa, S. Karasawa, M. Nakano, N. Koga, *Bull. Chem. Soc. Jpn.* **2006**, *79*, 1372–1382; b) S. Kanegawa, S. Karasawa, M. Nakano, N. Koga, *Chem. Commun.* **2004**, 1750–1751; c) S. Karasawa, K. Nakano, J.-i. Tanokashira, N. Yamamoto, T. Yoshizaki, N. Koga, *Dalton Trans.* **2012**, *41*, 13656–13667; d) S. Karasawa, D. Yoshihara, N. Watanabe, M. Nakano, N. Koga, *Dalton Trans.* **2008**, 1418–1420; e) S. Karasawa, N. Koga, *Inorg. Chem.* **2011**, *50*, 5186–5195; f) S. Karasawa, K. Nakano, D. Yoshihara, N. Yamamoto, J.-i. Tanokashira, T. Yoshizaki, Y. Inagaki, N. Koga, *Inorg. Chem.* **2014**, *53*, 5447–5457; g) S. Kanegawa, S. Karasawa, M. Maeyama, M. Nakano, N. Koga, *J. Am. Chem. Soc.* **2008**, *130*, 3079–3094; h) S. Karasawa, G. Zhou, H. Morikawa, N. Koga, *J. Am. Chem. Soc.* **2003**, *125*, 13676–13677; i) H. Tobinaga, M. Suehiro, T. Ito, G. Zhou, S. Karasawa, N. Koga, *Polyhedron* **2007**, *26*, 1905–1911.
- [11] W. Kaim, J. Fees, *Z. Naturforsch. B* **1995**, *50*, 123–127.
- [12] M. Glöckle, K. Hübler, H. J. Kümmerer, G. Denninger, W. Kaim, *Inorg. Chem.* **2001**, *40*, 2263–2269.
- [13] M. E. Lines, *J. Chem. Phys.* **1971**, *55*, 2977–2984.
- [14] O. Khan, *Molecular Magnetism*, VCH Publishers, New York, **1993**.
- [15] a) K. S. Cole, R. H. Cole, *J. Chem. Phys.* **1941**, *9*, 341–351; b) S. M. J. Aubin, Z. Sun, L. Pardi, J. Krzystek, K. Folting, L.-C. Brunel, A. L. Rheingold, G. Christou, D. N. Hendrickson, *Inorg. Chem.* **1999**, *38*, 5329–5340.
- [16] R. Orbach, *Proc. R. Soc. London Ser. A* **1961**, *264*, 458–484.

Received: May 4, 2015

Published online on June 12, 2015